


**Measuring the Dzyaloshinskii-Moriya interaction of the epitaxial Co/Ir(111) interface**Fabian Kloodd-Twesten <sup>\*</sup>, Susanne Kuhrau, Hans Peter Oepen, and Robert Frömter<sup>†</sup>*Universität Hamburg, Center for Hybrid Nanostructures, Luruper Chaussee 149, 22761 Hamburg, Germany*

(Received 4 January 2019; revised manuscript received 1 August 2019; published 5 September 2019)

The in-plane orientation of the magnetization in the center of domain walls is measured in Co/Ir(111) as a function of Co thickness via scanning electron microscopy with polarization analysis. Uncapped, thermally evaporated cobalt on an Ir(111) single-crystal surface is imaged *in situ* in ultrahigh vacuum. The initial pseudomorphic growth with an atomically flat interface of cobalt on iridium ensures comparability to theoretical calculations and provides a study of an interface that is as ideal as possible. Below a cobalt thickness of 8.8 monolayers, the magnetic domain walls are purely Néel oriented and show a clockwise sense of rotation. For larger thicknesses the plane of rotation changes and the domain walls show a significant Bloch-like contribution, allowing one to calculate the strength of the Dzyaloshinskii-Moriya interaction (DMI) from energy minimization. From the angle between the plane of rotation and the domain-wall normal an interfacial DMI parameter  $D_s = -(1.07 \pm 0.05)$  pJ/m is determined, which corresponds to a DMI energy per bond between two Co atoms at the interface of  $d_{\text{tot}} = -(1.04 \pm 0.05)$  meV.

DOI: [10.1103/PhysRevB.100.100402](https://doi.org/10.1103/PhysRevB.100.100402)**I. INTRODUCTION**

The Dzyaloshinskii-Moriya interaction (DMI) [1,2] is an antisymmetric exchange interaction that occurs due to the lack of inversion symmetry in a crystal structure (bulk type) or at the interface between two different materials (interface type). Caused by the spin-orbit interaction, the interfacial DMI reduces the energy of  $180^\circ$  domain walls between out-of-plane magnetized domains by initiating a laterally rotating spin configuration with a fixed sense of rotation. As a consequence, the domain-wall energy can even become negative in suitable materials, which results in a spin-spiral or skyrmion phase [3–7]. Recently, layered systems with a stacking of iridium, cobalt, and platinum have drawn a lot of attention [8–18] as they offer the possibility to stabilize magnetic skyrmions at room temperature (RT) [13]. *Ab initio* calculations of the ideally ordered Co/Ir(111) interface predict [8,9,19,20] that iridium induces a DMI of opposite sense of rotation of magnetization compared to platinum, resulting in a higher absolute DMI strength when cobalt is sandwiched between both materials. Unfortunately, the calculations yield conflicting results for the expected strength of the DMI. Such calculations are very sensitive to details of the band structure [20,21], the hybridization of the materials at the interface [20–22], the lattice-relaxation procedure, as well as the stacking of the lattice [23] and the assumed energy functional (i.e., considering first order in spin-orbit coupling [8,20,24,25], or accounting only for nearest-neighbor DMI [19,23]). Furthermore, extracting the DMI from a spin-spiral state makes it necessary to consider a reasonably small wave vector [21,25,26] ( $q \rightarrow 0$  in the micromagnetic limit) and hence calculations might result in

material-dependent errors when considering the energy of  $90^\circ$  spin spirals as in Refs. [9,19]. Despite these various sources of error, little is known about the actual reliability of the individual calculations.

Unfortunately, the authors of the three independent theoretical studies existing for Co/Ir(111) use different units and definitions, and do not compare their results. So, in the first place, a common description is required. Even though the DMI is an interface property, in micromagnetic calculations of thin, rigidly coupled films it is often treated as a scaled bulk property  $D_s/t$  where  $t$  is the thickness of the ferromagnetic material and  $D_s$  is the interfacial DMI constant [10,27–29]. In the following,  $D_s$  will be used for comparison between the different results. Definitions and conversions can be found in the Supplemental Material S1 [30] and were approved by the corresponding authors. Yang *et al.* investigated a bilayer system of 3 monolayers (ML) cobalt on 3 ML Ir(111) [9,19] and obtained  $D_s = -0.42$  pJ/m. Perini *et al.* calculated the DMI of 1 ML cobalt on 9 ML of Ir(111) and reported  $D_s = -1.10$  pJ/m [8]. Belabbes *et al.* give the highest DMI of  $D_s = -7.66$  pJ/m calculating 1 ML of cobalt on 6 ML of Ir(111) [20]. Even though all three published calculations agree in sign, they differ by more than an order of magnitude in size. This large discrepancy cannot be explained by the different amount of simulated cobalt layers, as Yang *et al.* [9,19] showed that the DMI depends particularly on the first monolayer and the contributions of the next layers are of minor relevance, resulting in the  $1/t$  dependence mentioned above.

Precise measurements of the DMI in a system comparable to theory are necessary to give insight into its microscopic origin and lead towards more reliable calculations. As the DMI is very sensitive to the interface quality, epitaxial films that wet the single-crystal surface and grow in a layer-by-layer fashion are best suited for this kind of investigation and ensure the previously mentioned comparability to theoretical calculations. In the case of Co/Ir(111) the first monolayer

<sup>\*</sup> Author to whom correspondence should be addressed: [fabian.kloodd@physik.uni-hamburg.de](mailto:fabian.kloodd@physik.uni-hamburg.de)

<sup>†</sup> Author to whom correspondence should be addressed: [rfroemte@physik.uni-hamburg.de](mailto:rfroemte@physik.uni-hamburg.de)

of thermally evaporated cobalt has been observed to grow pseudomorphically on the Ir(111) surface without intermixing [8,31,32], and an fcc stacking is supposed [8]. Therefore, this close-to-ideal system can be well compared to the system calculated in theory, in contrast to the more often studied sputtered film systems.

The spin-polarized scanning tunneling microscopy (SP-STM) study of Perini *et al.* [8] is performed on such a well-ordered interface, as a pseudomorphic cobalt monolayer on an Ir(111) single crystal is investigated. This experiment confirms the negative sign of  $D_s$  but gives no value for its strength [8]. Chen *et al.* publish a positive value of  $D_s = (0.37 \pm 0.09)$  pJ/m [33] for this interface; their quantitative analysis, however, appears to be based on inaccurate assumptions [34]. Further experimental reports of the DMI strength are only available for sputtered Co/Ir(111) interfaces but, due to the aforementioned problems, they show an even larger spread of values. They propose both negative [12,13] as well as positive [29,35,36] signs of the DMI, which is attributed to different interface properties [35,36] and is consequently no intrinsic property of the Co/Ir(111) interface. In conclusion, the sign of the DMI of the ideal system may be considered as known. However, the actual strength of the DMI is still an open question.

In the present study, the Dzyaloshinskii-Moriya interaction of the epitaxially grown Co/Ir(111) is measured by imaging the in-plane orientation of the magnetization within  $180^\circ$  domain walls (DWs) via scanning electron microscopy with polarization analysis (SEMPA). As DWs in a single uncovered Cobalt layer are investigated, the measured DMI can be unambiguously assigned to the Co/Ir(111) interface. A DMI contribution from the vacuum/Co interface is not to be expected [37]. In the absence of DMI, the magnetization of a DW rotates in the wall plane, reducing stray-field energy by avoiding magnetic volume charges, which is known as a Bloch wall. An additional interfacial DMI, favoring Néel-oriented DWs, tilts the rotational plane of the moments in the domain wall about the surface normal towards the normal of the DW. Therefore, the angle  $\Phi$  of the rotational plane with respect to the DW normal allows for analyzing the energy balance between the DMI and the stray-field energy, as long as both contributions are comparable in size [23,33,38–41]. In an illustrative picture,  $\Phi$  is the angle between the in-plane magnetization at the center of a DW with respect to the normal of the DW, which is why we denote it as angle of DW magnetization.  $\Phi$  is  $0^\circ$ ,  $180^\circ$  for a Néel orientation with clockwise, counterclockwise sense of rotation and  $-90^\circ$ ,  $+90^\circ$  for a Bloch orientation with clockwise, counterclockwise chirality, respectively.

## II. EXPERIMENT

SEMPA is well established as a magnetic imaging technique for the investigation of static magnetic structures ranging from hundreds of microns down to 3 nm in size [42]. It is a surface sensitive technique that measures two components of the magnetization simultaneously [43–45] with a depth of information of about 0.5 nm [42,46]. Recently, also the nanosecond magnetization dynamics became accessible [47–49]. The SEMPA system used here is sensitive to the in-plane spin polarization and allows for vectorial imaging

of the in-plane magnetization orientation with  $4^\circ$  precision for each pixel of an image [50], which is prerequisite for the investigation of the angle of DW magnetization [17,38,51].

The epitaxial Co/Ir(111) sample was prepared in a preparation chamber (base pressure of  $5 \times 10^{-11}$  mbar) directly attached to the SEMPA instrument. A clean, atomically flat Ir(111) surface was obtained by argon ion sputtering and periodic annealing of the bulk single-crystal substrate. The cleanliness of the surface was confirmed by Auger electron spectroscopy. Low-energy electron diffraction revealed a sharp  $p(1 \times 1)$  pattern. Subsequently, a wedge-shaped cobalt film was evaporated at RT. As the uncertainty in cobalt thickness is the leading term in the accuracy of DMI determination, a thorough calibration of the evaporation rate was performed. In this way, an effective “magnetic” thickness is obtained, which makes the analysis less dependent on growth-related variations of film density. The sample preparation is described in detail in Supplemental Material S2 [30].

## III. RESULTS AND DISCUSSION

Magnetic domain patterns of several cobalt films were recorded within a thickness range of 3.5–17 ML. At lower thicknesses the as-grown cobalt films show an out-of-plane magnetized multidomain state. At  $(9.7 \pm 0.3)$  ML the spin-reorientation transition (SRT) towards easy plane sets in, which proceeds via magnetization canting [52]. Here, higher-order terms of the anisotropy needed to be considered in the analysis [53,54], which is beyond the scope of this article. Therefore, only data significantly below the onset of the SRT will be analyzed. Starting from 7.1-ML cobalt thickness, DWs could be resolved with sufficient accuracy to extract angles of DW magnetization from the SEMPA micrographs. For cobalt thicknesses below 7.1 ML the DWs were too narrow to be adequately imaged. In the lower thickness range, magnetic domains with out-of-plane orientation could still be imaged by slightly tilting the sample, demonstrating that the cobalt layer is ferromagnetic at least down to 3.5 ML.

The magnetic domain structure of 8.6 ML cobalt is displayed in Fig. 1. Panels (a) and (b) show the vertical and horizontal in-plane component of the magnetization, respectively. A slight sample tilt of  $10^\circ$  about the horizontal axis ensures that a small projection of the out-of-plane component is visible in the vertical component image (a), which allows us to derive the sense of rotation in the DWs. Figure 2(c) gives a full three-dimensional map of the magnetization. The up (black)/down (white) domain contrast is obtained from the contribution of the perpendicular domains observed in Fig. 1(a). The in-plane orientation of the domain-wall magnetization is color coded according to the color wheel in the lower left corner. It is calculated from the individual component images 1(a) and 1(b). The data show Néel-oriented DWs with a fixed, clockwise sense of rotation (see sketch for definition). This finding is in agreement with recent SP-STM investigations of the cobalt monolayer on Ir(111) [8] and is evidence of a negative DMI. Further inspection via line profiles in Fig. 1 yields that at this thickness the DWs are purely Néel oriented ( $\Phi = 0^\circ$ ) and thus only a lower threshold for the DMI strength can be derived.

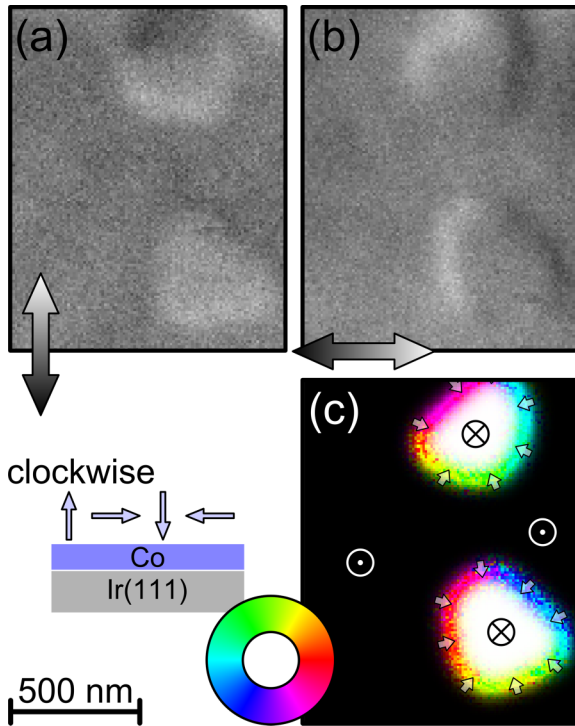


FIG. 1. Magnetic domain structure of a 8.6-ML cobalt film grown on the Ir(111) single-crystal surface. (a) and (b) display the vertical and horizontal in-plane components of the spin polarization. Due to a sample tilt of  $10^\circ$  about the horizontal axis an additional projection of the out-of-plane magnetization component is visible in the vertical component image (a). From the raw data a complete three-dimensional map of the magnetization vector is assembled in (c). The black and white contrast indicates domains pointing up and down, respectively. The magnetization components in the film plane are color coded according to the given color wheel. Domains pointing into and out of the surface are separated by Néel-oriented domain walls with clockwise sense of rotation.

A value of the DMI strength can be obtained when the domain wall starts to tilt towards a Bloch wall at higher cobalt thickness. Figure 2(a) shows a line scan across two DWs at a Co thickness of 9.0 ML. Blue circles and red squares correspond to the horizontal (left axis) and vertical (right axis) component of the in-plane magnetization, respectively. The error bars are calculated based on the Poisson statistics of the individual electron count per channel, as described in Ref. [50]. The corresponding SEMPA micrograph in Fig. 2(b) (horizontal component shown) was recorded beforehand and used to select the position of the line scan, which is marked in blue. In Fig. 2(c) a sketch illustrates the definition of the in-plane angle of magnetization within the DW with respect to its normal.

As the apparent width of the DWs is obviously dominated by the instrumental resolution, a Gaussian profile is expected that originates from the shape of the primary beam. The profiles of both magnetization components are analyzed in a single fit procedure comprising two independent Gaussian profiles for the two DWs for each component. While the integrated intensities of the horizontal and vertical components are independent parameters for each Gaussian, the standard deviation (or the width) and the position are shared (see Supplemental Material S3 [30]). A remaining contribution from the out-of-plane domains has been included in the fit using a Gaussian error function. This out-of-plane contribution is already corrected in the given data. It corresponds to a  $5^\circ$  tilt for this image, which has only a negligible influence on the in-plane domain contrast [38]. The DW to the right-hand side (marked in purple in the inset) is oriented within an uncertainty of  $2^\circ$  along the image vertical. For this reason, the horizontal magnetization component directly reflects the Néel contribution to the rotation of the DW, while the vertical component gives the Bloch contribution. It is clearly visible that at this investigated thickness the DW is mainly but not purely Néel oriented. From the ratio of the respective integrated intensities of the Gaussians a DW magnetization angle

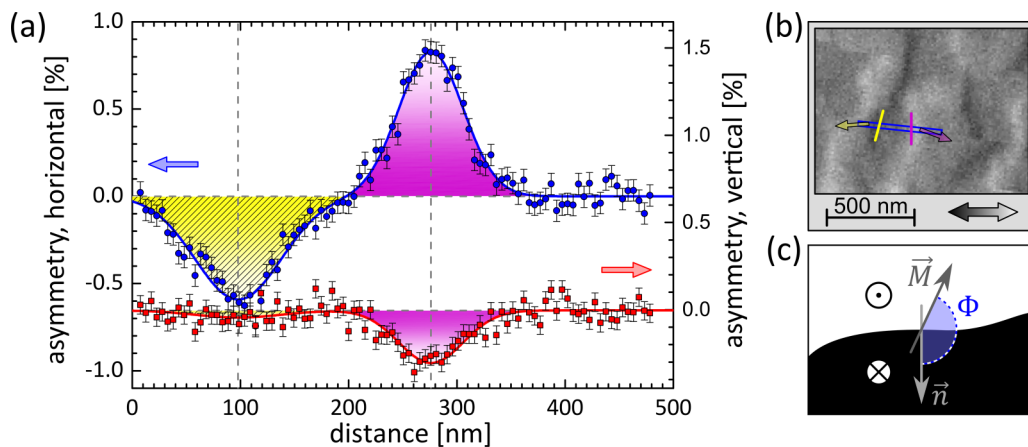


FIG. 2. (a) Line scan across two domain walls at 9.0 ML cobalt thickness. Blue circles and red squares correspond to the horizontal (left axis) and vertical (right axis) components of the in-plane magnetization. In (b) an overview image of the horizontal magnetization component is shown that was recorded beforehand and used to position the line scan. The DWs marked in yellow and purple correspond to the shading of the Gaussian profiles and the arrows indicate the extracted DW magnetizations. Both DWs are not purely Néel-oriented and show opposite Bloch rotations, yielding angles of DW magnetization of about  $\pm 20^\circ$ . Panel (c) illustrates the definition of this angle  $\Phi$  between the magnetization vector  $\vec{M}$  in the center of a DW and the normal  $\vec{n}$  of the DW.

$\Phi = -(20.1 \pm 2.6)^\circ$  is calculated. The situation is different for the DW to the left (yellow) that is rotated by  $(15 \pm 5)^\circ$  with respect to the image vertical. Within experimental accuracy, the vertical magnetization component is close to zero, which means that the DW magnetization is aligned with the horizontal axis. An analysis of the fit yields an angle of  $(18.8 \pm 5.5)^\circ$ . The errors for both angles of DW magnetization mainly originate from the uncertainty in determining the local wall orientation and not from the magnetization orientation. Although both angles have opposite signs, they give a consistent picture, as the energy minimization that involves stray-field energy and DMI only defines the absolute value and not the sign of  $\Phi$ . Contrary to the DMI, which favors only one Néel orientation, both Bloch orientations are degenerate in energy, which is consistent with recent studies on other materials [39–41].

The different widths visible in the Gaussian fits can be attributed to astigmatism of the scanning electron beam, yielding different convolutions depending on the orientation of line-like objects (see Supplemental Material S3 [30]). However, the integral intensities  $V$  are not influenced by this effect as they depend only on the actual DW width and the in-plane contrast and make a precise measurement of the angle of DW magnetization possible [38]. In good agreement, one obtains  $V = (0.65 \pm 0.03)$  nm for the left DW and  $V = (0.61 \pm 0.06)$  nm for the right DW, which leads to a DW width according to the definition by Lilley [55] of  $d_w = (14.6 \pm 0.7)$  nm.

#### IV. DETERMINING THE DMI STRENGTH

By minimizing the energy of a DW including DMI and stray-field energy via micromagnetic modeling, the DMI parameter  $D_s$  can be determined from comparison to the measured equilibrium angle of DW magnetization. The main problem in modeling is to determine the stray-field energy of the magnetic volume charges accurately. This energy can be obtained numerically [33,39–41] or using an analytical approximation [56–58]. In this study, the measured angles of DW magnetization are matched with micromagnetic simulations of DWs using MicroMagnum [59]. For comparison, also the analytical models are fitted to the experimental data.

In Fig. 3 a plot of the angle of DW magnetization as function of the cobalt thickness is shown (gray circles), together with further data points, that have been obtained in the same way as in Fig. 2 at different thicknesses. For lower cobalt thickness the walls show within the error margin an angle of  $\Phi = 0^\circ$ , corresponding to purely Néel-oriented walls with a clockwise sense of rotation. Above a cobalt thickness of 8.8 ML, DWs that are not purely Néel-oriented are observed. The red squares in Fig. 3 correspond to micromagnetic simulations of DWs using a DMI parameter of  $D_s = -1.065 \frac{\text{pJ}}{\text{m}}$  (details on the simulations in Supplemental Material S5 [30]). In a next step, we varied the value of  $D_s$  in the simulations (not shown) to find the uncertainty in fitting our experimental results. We obtain  $D_s = -(1.07 \pm 0.01) \frac{\text{pJ}}{\text{m}}$ . An additional and independent analysis has been performed by fitting the approximate solution developed by Lemesh *et al.* [58] (details for the analysis in Supplemental Material S4 [30]) with  $D_s$  as only fit parameter. This fit yields  $D_s = -(1.04 \pm 0.01) \frac{\text{pJ}}{\text{m}}$

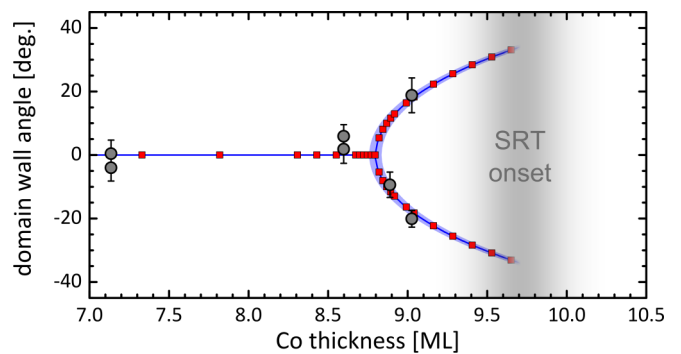


FIG. 3. Measured angles of the DW magnetization as function of cobalt thickness (gray circles). Below a cobalt thickness of 8.8-ML purely Néel-oriented domain walls are observed that correspond to a clockwise sense of rotation. Above, the domain walls show a significant Bloch contribution until the SRT sets in at  $(9.7 \pm 0.3)$  ML. The measured angles match with micromagnetic simulations of DWs using a DMI strength of  $D_s = -1.07$  pJ/m (red squares). A fit of the approximating equation of Lemesh *et al.* [58] results in a similar value of  $D_s = -(1.04 \pm 0.01)$  pJ/m (blue line). The blue shaded region visualizes the confidence band at  $1 \sigma$ .

and is shown in blue with a blue shade visualizing the confidence interval at  $1 \sigma$ . Lemesh *et al.* interpolate between the solutions for ultrathin (previously given by Tarasenko *et al.* [56]) and thick films giving a better match than the ultrathin film solution. Using directly the latter, as in Refs. [38,60], results in an overestimation of the DMI strength by 10%.

In addition to the small statistical error margin in the DMI parameter  $D_s$ , a systematic error caused by the thickness calibration of the evaporated Co has to be considered (see Supplemental Material S2 [30]). Accounting for 2.1% uncertainty in the thickness calibration, which results from calibration by atomic force microscopy, one obtains

$$D_s = -(1.07 \pm 0.05) \frac{\text{pJ}}{\text{m}}.$$

Converting this continuum-model value into an atomic DMI strength [37] results in  $d_{\text{tot}} = -(1.04 \pm 0.05)$  meV per bond, where the total DMI strength is referenced to the interface cobalt layer only (see Supplemental Material S1 [30]).

In conclusion, SEMPA is used to determine the strength of the Dzyaloshinskii-Moriya interaction of the epitaxially grown Co/Ir(111) interface. The growth and preparation conditions ensure an ideal interface between Co and Ir, making the experimentally determined DMI strength comparable to those from published *ab initio* calculations. Below a thickness of 8.8 ML, purely Néel-oriented DW with a clockwise sense of rotation are observed. Above this thickness the stray-field contribution shifts the energy minimum towards a partial Bloch orientation of the DW, giving access to the strength of the DMI. Together with our earlier investigation of the DMI at the Co/Pt(111) interface [38], we verify the opposing signs of the DMI at the Co/Ir(111) and Co/Pt(111) interfaces, at least for the ideal systems, which is in agreement with the calculations and in contrast to the findings in Refs. [29,33,35,36]. The determined DMI strength matches the value calculated in Perini *et al.* [8], but

significantly deviates from the smaller and larger values given in Refs. [9,19,20].

### ACKNOWLEDGMENTS

We acknowledge financial support by the DFG within SFB 668. The authors thank S. Meyer, B. Dupé, L. Rózsa, and

A. Manchon for fruitful discussions regarding the conversion between different DMI definitions, C. Heyn for thickness calibration via atomic force microscopy, K. Litzius for sharing a MicroMagnum version that includes the Dzyaloshinskii-Moriya interaction, P. Bayat for additional energy dispersive x-ray spectroscopy, and K. von Bergmann for information regarding the growth of cobalt on Ir(111).

- [1] I. E. Dzialoshinskii, Zh. Eksp. Teor. Fiz. **32**, 1547 (1957) [*Sov. Phys. JETP* **5**, 1259 (1957)].
- [2] T. Moriya, *Phys. Rev.* **120**, 91 (1960).
- [3] E. Y. Vedmedenko, L. Udvardi, P. Weinberger, and R. Wiesendanger, *Phys. Rev. B* **75**, 104431 (2007).
- [4] M. Bode, M. Heide, K. von Bergmann, P. Ferriani, S. Heinze, G. Bihlmayer, A. Kubetzka, O. Pietzsch, S. Blügel, and R. Wiesendanger, *Nature (London)* **447**, 190 (2007).
- [5] S. Heinze, K. von Bergmann, M. Menzel, J. Brede, A. Kubetzka, R. Wiesendanger, G. Bihlmayer, and S. Blügel, *Nat. Phys.* **7**, 713 (2011).
- [6] S. Rohart and A. Thiaville, *Phys. Rev. B* **88**, 184422 (2013).
- [7] N. Romming, C. Hanneken, M. Menzel, J. E. Bickel, B. Wolter, K. von Bergmann, A. Kubetzka, and R. Wiesendanger, *Science* **341**, 636 (2013).
- [8] M. Perini, S. Meyer, B. Dupé, S. von Malottki, A. Kubetzka, K. von Bergmann, R. Wiesendanger, and S. Heinze, *Phys. Rev. B* **97**, 184425 (2018).
- [9] H. Yang, O. Boulle, V. Cros, A. Fert, and M. Chshiev, *Sci Rep.* **8**, 12356 (2018).
- [10] D.-S. Han, N.-H. Kim, J.-S. Kim, Y. Yin, J.-W. Koo, J. Cho, S. Lee, M. Kläui, H. J. M. Swagten, B. Koopmans, and C.-Y. You, *Nano Lett.* **16**, 4438 (2016).
- [11] S. Kuhrau, F. Klodt-Twesten, C. Heyn, H. P. Oepen, and R. Frömter, *Appl. Phys. Lett.* **113**, 172403 (2018).
- [12] A. Hrabec, N. A. Porter, A. Wells, M. J. Benitez, G. Burnell, S. McVitie, D. McGrouther, T. A. Moore, and C. H. Marrows, *Phys. Rev. B* **90**, 020402(R) (2014).
- [13] C. Moreau-Luchaire, C. Moutafis, N. Reyren, J. Sampaio, C. A. F. Vaz, N. V. Horne, K. Bouzehouane, K. Garcia, C. Deranlot, P. Warnicke, P. Wohlhüter, J.-M. George, M. Weigand, J. Raabe, V. Cros, and A. Fert, *Nat. Nanotechnol.* **11**, 444 (2016).
- [14] J. Lucassen, F. Klodt-Twesten, R. Frömter, H. P. Oepen, R. A. Duine, H. J. Swagten, B. Koopmans, and R. Lavrijsen, *Appl. Phys. Lett.* **111**, 132403 (2017).
- [15] G. Ziemys, V. Ahrens, S. Mendisch, G. Csaba, and M. Becherer, *AIP Adv.* **8**, 056310 (2018).
- [16] M. Bacani, M. A. Marioni, J. Schwenk, and H. J. Hug, *Sci. Rep.* **9**, 3114 (2019).
- [17] J. Lucassen, M. J. Meijer, F. Klodt-Twesten, R. Frömter, O. Kurnosikov, R. A. Duine, H. J. M. Swagten, B. Koopmans, and R. Lavrijsen, *arXiv:1904.01898*.
- [18] J. Lucassen, C. F. Schippers, L. Rutten, R. A. Duine, H. J. M. Swagten, B. Koopmans, and R. Lavrijsen, *Appl. Phys. Lett.* **115**, 012403 (2019).
- [19] H. Yang, A. Thiaville, S. Rohart, A. Fert, and M. Chshiev, *Phys. Rev. Lett.* **118**, 219901(E) (2017).
- [20] A. Belabbes, G. Bihlmayer, F. Bechstedt, S. Blügel, and A. Manchon, *Phys. Rev. Lett.* **117**, 247202 (2016).
- [21] L. M. Sandratskii, *Phys. Rev. B* **96**, 024450 (2017).
- [22] V. Kashid, T. Schena, B. Zimmermann, Y. Mokrousov, S. Blügel, V. Shah, and H. G. Salunke, *Phys. Rev. B* **90**, 054412 (2014).
- [23] G. J. Vida, E. Simon, L. Rózsa, K. Palotás, and L. Szunyogh, *Phys. Rev. B* **94**, 214422 (2016).
- [24] M. Heide, G. Bihlmayer, and S. Blügel, *Physica B* **404**, 2678 (2009).
- [25] B. Dupé, M. Hoffmann, C. Paillard, and S. Heinze, *Nat. Commun.* **5**, 4030 (2014).
- [26] B. Zimmermann, G. Bihlmayer, M. Böttcher, M. Bouhassoune, S. Lounis, J. Sinova, S. Heinze, S. Blügel, and B. Dupé, *Phys. Rev. B* **99**, 214426 (2019).
- [27] J. Cho, N.-H. Kim, S. Lee, J.-S. Kim, R. Lavrijsen, A. Solognac, Y. Yin, D.-S. Han, N. J. J. van Hoof, H. J. M. Swagten, B. Koopmans, and C.-Y. You, *Nat. Commun.* **6**, 7635 (2015).
- [28] M. Belméguenai, J.-P. Adam, Y. Roussigné, S. Eimer, T. Devolder, J.-V. Kim, S. M. Cherif, A. Stashkevich, and A. Thiaville, *Phys. Rev. B* **91**, 180405(R) (2015).
- [29] N.-H. Kim, J. Jung, J. Cho, D.-S. Han, Y. Yin, J.-S. Kim, H. J. M. Swagten, and C.-Y. You, *Appl. Phys. Lett.* **108**, 142406 (2016).
- [30] See Supplemental Material at <http://link.aps.org/supplemental/10.1103/PhysRevB.100.100402> for details on the conversion between different DMI calculations, the sample preparation, and the analysis of the domain-wall profiles measured by SEMPA (see, also, Refs. [61–68] therein).
- [31] J. E. Bickel, F. Meier, J. Brede, A. Kubetzka, K. von Bergmann, and R. Wiesendanger, *Phys. Rev. B* **84**, 054454 (2011).
- [32] J. Drnec, S. Vlaic, I. Carlomagno, C. J. Gonzalez, H. Isern, F. Carlà, R. Fiala, N. Rougemaille, J. Coraux, and R. Felici, *Carbon* **94**, 554 (2015).
- [33] G. Chen, A. T. N'Diaye, Y. Wu, and A. K. Schmid, *Appl. Phys. Lett.* **106**, 062402 (2015).
- [34] The value of  $D$  published in Ref. [33] is derived based on the assumption of an abrupt transition between Néel and Bloch walls at a critical thickness, which is inconsistent with the findings from our experiment, as well as with micromagnetic modeling. This differing data analysis, however, cannot account for the oppositely reported sign of  $D$ .
- [35] K. Shahbazi, J.-V. Kim, H. T. Nembach, J. M. Shaw, A. Bischof, M. D. Rossell, V. Jeudy, T. A. Moore, and C. H. Marrows, *Phys. Rev. B* **99**, 094409 (2019).
- [36] F. Ajejas, V. Krizáková, D. de Souza Chaves, J. Vogel, P. Perna, R. Guerrero, A. Gudin, J. Camarero, and S. Pizzini, *Appl. Phys. Lett.* **111**, 202402 (2017).
- [37] H. Yang, A. Thiaville, S. Rohart, A. Fert, and M. Chshiev, *Phys. Rev. Lett.* **115**, 267210 (2015).

- [38] E. C. Corredor, S. Kuhrau, F. Kloodt-Twesten, R. Frömter, and H. P. Oepen, *Phys. Rev. B* **96**, 060410(R) (2017).
- [39] G. Chen, T. Ma, A. T. N'Diaye, H. Kwon, C. Won, Y. Wu, and A. K. Schmid, *Nat. Commun.* **4**, 2671 (2013).
- [40] H. Yang, G. Chen, A. A. C. Cotta, A. T. N'Diaye, S. A. Nikolaev, E. A. Soares, W. A. A. Macedo, K. Liu, A. K. Schmid, A. Fert, and M. Chshiev, *Nat. Mater.* **17**, 605 (2018).
- [41] G. Chen, J. Zhu, A. Quesada, J. Li, A. T. N'Diaye, Y. Huo, T. P. Ma, Y. Chen, H. Y. Kwon, C. Won, Z. Q. Qiu, A. K. Schmid, and Y. Z. Wu, *Phys. Rev. Lett.* **110**, 177204 (2013).
- [42] K. Koike, *Microscopy* **62**, 177 (2013).
- [43] K. Koike and K. Hayakawa, *Jpn. J. Appl. Phys.* **23**, L187 (1984).
- [44] J. Unguris, D. T. Pierce, and R. J. Celotta, *Rev. Sci. Instrum.* **57**, 1314 (1986).
- [45] H. P. Oepen and J. Kirschner, *J. Phys. Colloq.* **49**, C8-1853 (1988).
- [46] R. Frömter, E. C. Corredor, S. Hankemeier, F. Kloodt-Twesten, S. Kuhrau, F. Lofink, S. Rößler, and H. P. Oepen, *Imaging the Interaction of Electrical Currents with Magnetization Distributions*, in *Atomic- and Nanoscale Magnetism*, edited by R. Weisendanger (Springer, Cham, 2018).
- [47] R. Frömter, F. Kloodt, S. Rößler, A. Frauen, P. Staeck, D. R. Cavicchia, L. Bocklage, V. Röbisch, E. Quandt, and H. P. Oepen, *Appl. Phys. Lett.* **108**, 142401 (2016).
- [48] F. Kloodt-Twesten, S. Kuhrau, P. Staeck, D. R. Cavicchia, F. Lofink, H. P. Oepen, and R. Frömter, *Phys. Rev. B* **97**, 024426 (2018).
- [49] D. Schönke, A. Oelsner, P. Krautscheid, R. M. Reeve, and M. Kläui, *Rev. Sci. Instrum.* **89**, 083703 (2018).
- [50] R. Frömter, S. Hankemeier, H. P. Oepen, and J. Kirschner, *Rev. Sci. Instrum.* **82**, 033704 (2011).
- [51] B. Boehm, A. Bisig, A. Bischof, G. Stefanou, B. J. Hickey, and R. Allenspach, *Phys. Rev. B* **95**, 180406(R) (2017).
- [52] A. D. Vu, J. Coraux, G. Chen, A. T. N'Diaye, A. K. Schmid, and N. Rougemaille, *Sci. Rep.* **6**, 24783 (2016).
- [53] D. Stickler, R. Frömter, H. Stillrich, C. Menk, H. P. Oepen, C. Gutt, S. Streit-Nierobisch, L.-M. Stadler, G. Grübel, C. Tieg, and F. Yakhou-Harris, *Phys. Rev. B* **84**, 104412 (2011).
- [54] H. P. Oepen, M. Speckmann, Y. Millev, and J. Kirschner, *Phys. Rev. B* **55**, 2752 (1997).
- [55] B. Lilley, *Philos. Mag.* **41**, 792 (1950).
- [56] S. V. Tarasenko, A. S. V. V. Tarasenko, and J. Ferré, *J. Magn. Magn. Mater.* **189**, 19 (1998).
- [57] F. Büttner, B. Krüger, S. Eisebitt, and M. Kläui, *Phys. Rev. B* **92**, 054408 (2015).
- [58] I. Lemesch, F. Büttner, and G. S. D. Beach, *Phys. Rev. B* **95**, 174423 (2017).
- [59] C. Abert, A. Drews, B. Krüger, and G. Selke, *MicroMagnum*, Vol. 0.2 (2016).
- [60] As our own analysis in Ref. [38] is based on the solution for ultrathin films. The determined lower threshold is stated 10% to high. For the upper threshold, however, the thin-film limit applies, and this value remains unaffected by this correction.
- [61] A. Thiaville, S. Rohart, E. Jue, V. Cros, and A. Fert, *Europhys. Lett.* **100**, 57002 (2012).
- [62] L. E. Davis, N. C. MacDonald, P. W. Palmberg, G. E. Riach, and R. E. Weber, *Handbook of Auger Electron Spectroscopy: A Reference Book of Standard Data for Identification and Interpretation of Auger Electron Spectroscopy Data* (Physical Electronics Division, Perkin-Elmer, Waltham, MA, 1976).
- [63] A. Hubert and R. Schäfer, *Magnetic Domains: The Analysis of Magnetic Microstructures* (Springer, Berlin, 2009).
- [64] M. B. Stearns, *Landolt-Börnstein New Series III/19a*, Vol. 19a (Springer-Verlag, Berlin, 1986).
- [65] F. Meier, K. von Bergmann, P. Ferriani, J. Wiebe, M. Bode, K. Hashimoto, S. Heinze, and R. Wiesendanger, *Phys. Rev. B* **74**, 195411 (2006).
- [66] M. Perini, Nanoscale noncollinear magnetic structures in Co-based epitaxial ultrathin films, Ph.D. thesis, Universität Hamburg, 2018.
- [67] K. Litzius, I. Lemesch, B. Krüger, L. Caretta, K. Richter, F. Büttner, P. Bassirian, J. Förster, R. M. Reeve, M. Weigand, I. Bykova, H. Stoll, G. Schütz, G. S. D. Beach, and M. Kläui, *Nat. Phys.* **13**, 170 (2017).
- [68] M. D. DeJong and K. L. Livesey, *Phys. Rev. B* **95**, 054424 (2017).